

# Urban water storage capacity inferred from observed evapotranspiration recession

H.J. Jongen<sup>1,2</sup>, G-J. Steeneveld<sup>2</sup>, J. Beringer<sup>3</sup>, A. Christen<sup>4</sup>, K. Fortuniak<sup>5</sup>, J. Hong<sup>6</sup>, J-W. Hong<sup>7</sup>, C.M.J. Jacobs<sup>8</sup>, L. Järvi<sup>9,10</sup>, F. Meier<sup>11</sup>, W. Pawlak<sup>5</sup>, M. Roth<sup>12</sup>, N.E. Theeuwes<sup>13,14</sup>, E. Velasco<sup>15</sup>, and A.J. Teuling<sup>1</sup>

<sup>1</sup>Hydrology and Quantitative Water Management, Wageningen University, Wageningen, The Netherlands.

<sup>2</sup>Meteorology and Air Quality, Wageningen University, Wageningen, The Netherlands.

<sup>3</sup>School of Agriculture and Environment, University of Western Australia, Crawley, Australia.

<sup>4</sup>Chair of Environmental Meteorology, Faculty of Environment and Natural Resources, University of Freiburg, Freiburg, Germany

<sup>5</sup>Department of Meteorology and Climatology, Faculty of Geographical Sciences, University of Łódź, Łódź, Poland.

<sup>6</sup>Department of Atmospheric Sciences, Yonsei University, Seoul, South Korea.

<sup>7</sup>Korean Environment Institute, Sejong, South Korea.

<sup>8</sup>Wageningen Environmental Research, Wageningen University and Research, Wageningen, The Netherlands.

\*

<sup>9</sup>Institute for Atmospheric and Earth System Research / Physics, University of Helsinki, Helsinki, Finland.

<sup>10</sup>Helsinki Institute of Sustainability Science, University of Helsinki, Helsinki, Finland.

<sup>11</sup>Chair of Climatology, Technische Universität Berlin, Berlin, Germany.

<sup>12</sup>Department of Geography, National University of Singapore, Singapore.

<sup>13</sup>Department of Meteorology, University of Reading, Reading, United Kingdom.

<sup>14</sup>Royal Netherlands Meteorological Institute (KNMI), De Bilt, The Netherlands.

<sup>15</sup>Independent Research Scientist, Singapore.

## Key Points:

- A new method is proposed to infer urban water storage capacity from evapotranspiration recession.
- Rapid decline of evapotranspiration after rainfall at all sites reflects strong water-limitation.
- Water storage capacity in cities is an order of magnitude smaller than in rural and forested areas.

---

\*Current affiliation: National Institute for Public Health and the Environment (RIVM), Bilthoven, The Netherlands

Corresponding author: Harro Jongen, [harro.jongen@wur.nl](mailto:harro.jongen@wur.nl)

## Abstract

Water storage plays an important role in mitigating heat and flooding in urban areas. Assessment of the capacity of cities to store water remains challenging due to the extreme heterogeneity of the urban surface. Traditionally, effective storage has been estimated from runoff. Here, we present a novel approach to estimate water storage capacity from recession rates of evaporation during precipitation-free periods. We test this approach for cities at neighborhood scale with eddy-covariance latent heat flux observations from thirteen contrasting sites with different local climate zones, vegetation cover and characteristics, and climates. We find effective water storage capacities to vary between 1.5 and 20 mm corresponding to  $e$ -folding timescales of 2.5 to 12 days. According to our results, urban water storage capacity is at least one order of magnitude smaller than the observed values for natural ecosystems, resulting in an evaporation regime characterised by extreme water limitation.

## Plain Language Summary

Urban water storage plays an important role in mitigating urban flooding and affects urban heat via cooling through evapotranspiration. Determining the amount of water that can be stored in a city remains challenging due to the variability in urban landscapes. The methodology presented estimates this water storage based on how evapotranspiration declines over time during periods without precipitation. The estimated storage capacities amount to 1.5–20 mm, which is an order of magnitude smaller than in natural ecosystems.

## 1 Introduction

Cities face weather-related risks magnified by climate change, such as heatwaves and flooding (Wilby, 2007). At the same time, urbanization is expected to further increase the already large share of the world population living in those cities to 68% in 2050 (United Nations, 2018). As for heatwaves, global temperatures are projected to increase, with the high temperatures exacerbated in urban areas where air temperatures are typically higher than in the rural surroundings due to the Urban Heat Island effect (UHI) (Oke, 1982; Santamouris, 2014; Oke et al., 2017). These high temperatures in cities lead to increased energy demands, health issues and excess mortality (Stone Jr & Rodgers, 2001; Gabriel & Endlicher, 2011; Laaidi et al., 2011; Santamouris, 2015; Gasparrini et al., 2017). The UHI originates from the difference between the rural and urban energy balances due to lower albedo, less vegetation, higher heat storage capacity and anthropogenic heat release in cities (Oke, 1982). By endorsing a higher latent heat flux via the evaporation of water complemented by shading, urban vegetation is often given a central role in attempts to reduce the UHI (Ennos, 2010). Indeed, higher vegetation fractions are associated with lower urban air and canopy temperatures (e.g. Gallo et al., 1993; Weng et al., 2004; Theeuwes et al., 2017), although in specific situations vegetation can cause higher temperatures (Meili et al., 2021a). It has been shown that actively expanding the vegetation fraction as part of urban renewal indeed has the potential to mitigate the UHI (Wei & Shu, 2020). Since vegetation-mediated cooling strongly depends on water availability for evapotranspiration (ET) (Avisar, 1992), there is a need for methods to analyze and evaluate the effective storage in urban environments.

Urban areas not only alter the surface energy partitioning, but affect the water balance and make cities more prone to flooding. The high impervious surface fraction in cities results in more storm water being discharged as runoff in urban areas, which on top of that accumulates faster (Arnold Jr & Gibbons, 1996; Fletcher et al., 2013). Consequently, urbanization decreases water availability for ET and thus indirectly contributes to the UHI (Taha, 1997; Zhao et al., 2014), and together with heavy rainfall events leads to annual flood volumes that are 2–9 times higher than in rural areas (Paul & Meyer,

2001; Hamdi et al., 2011; Zhou et al., 2019). Due to the high population density and concentration of capital in cities, these floods cause considerable damage (Tingsanchali, 2012). Floods and the associated damage are likely to be further increased by the ongoing intensification of the water cycle expressed in among other things more precipitation (Huntington, 2006). Solutions have been proposed under various names such as Water Sensitive Urban Design (WSUD) (Wong, 2006), Low Impact Development (LID) (Qin et al., 2013), Sustainable Drainage Systems (SWS) (Zhou, 2014) and sponge cities (Gaines, 2016). The common ground of these concepts is their focus on increasing infiltration and effective storage capacity, of which the latter at urban landscape scale is crucial for their performance (Graham et al., 2004; Qin et al., 2013). Therefore, an evaluation of the effective storage in urban environments is also needed in the light of flooding events.

Estimating the water storage capacity remains challenging, as water sources for ET in urban landscapes are spatially heterogeneous (Sailor, 2011). Previous studies have focused on ET from individual sources (e.g. Gash et al., 2008; Starke et al., 2010; Pataki et al., 2011; Ramamurthy & Bou-Zeid, 2014), as well as on their combined behaviour at street or neighborhood scale (e.g. Christen & Vogt, 2004; Jacobs et al., 2015; Meili et al., 2020, 2021b). In order to study ET on a neighborhood scale (order of hundreds of meters to 1–2 kilometers), flux measurements of latent heat with an associated footprint, such as those obtained by eddy covariance or scintillometry, are becoming increasingly popular. Examples of cities for which these measurements have been taken and analyzed are Arnhem (Jacobs et al., 2015), Basel (Christen & Vogt, 2004), Helsinki (Vesala et al., 2008), Melbourne (Coutts et al., 2007b), Seoul (Hong et al., 2019) and Singapore (Roth et al., 2017). These measurement sites are chosen such that their footprint covers an area as homogeneous as possible to enable research on the influence of the city design on the surface energy balance partitioning. ET originates from the urban water storage, so ET observations contain information on this storage. However, the link between neighborhood-scale observations and urban water storage has not been exploited, despite the relevance of this water storage.

The concept providing this link between neighborhood-scale ET observations and urban water storage is a recession analysis of the observed ET. From the 1970s, recession analysis has an extensive track record in groundwater and hill slope hydrology linking discharge to water storage (e.g. Brutsaert & Nieber, 1977; Kirchner, 2009; Troch et al., 2013). Similarly, daily ET can be linked to water storage during a drydown, a period without precipitation creating water-limited conditions. Recession analysis of ET decay reveals the timescale over which ET declines by 63% (*e*-folding time), and reflects the available storage and resilience to droughts (Wetzel & Chang, 1987; Salvucci, 2001; Saleem & Salvucci, 2002). The reflected storage is defined by the methodology as the dynamic water storage capacity available to the atmosphere for ET, which includes soil moisture, intercepted precipitation and open water varying from lakes to puddles. In studies using daily ET over natural ecosystems, Teuling et al. (2006) and Boese et al. (2019) found timescales ranging from 15 days for short vegetation to 35 days for forest ecosystems, and corresponding storage capacities in the range between 30 and 200 mm, with most sites in the range of 50 to 100 mm. A similar analysis at the global scale by McColl et al. (2017) determined that the timescales of drydowns in surface soil moisture with satellite imagery on 36 km resolution and found timescales ranging from 2 to 20 days. Although valuable insight can be obtained from a comparison of urban and rural ET dynamics, recession analysis has not yet been applied to urban ET.

In this study, we test and adjust the methodology developed to estimate water storage capacity based on observations of daily ET in natural ecosystems for application in urban environments. This allows us to infer dynamic water storage capacities at the neighborhood-scale from latent flux observations that provide ET from eddy-covariance flux towers. The methodology is tested for neighbourhoods in different cities located across a range of climate conditions and with different urban land cover and structure, which are both

136 likely to affect the storage capacity. The results from the different cities are compared  
 137 to each other to quantify the effect of the site characteristics (e.g. vegetation fraction)  
 138 on the water storage, and to natural ecosystems for quantification of the effect of urban-  
 139 ization.

## 140 2 Data and Methods

141 We analyze latent heat fluxes and auxiliary meteorological data obtained from eddy  
 142 covariance flux towers at thirteen sites in eleven different cities to estimate water stor-  
 143 age. Table 1 lists the most important characteristics of each site, including the Köppen-  
 144 Geiger climate and local climate zones as described by Stewart and Oke (2012), and key  
 145 references. In these references, all observation sites and measurement details are fully  
 146 described. The sites were chosen based on the length of the data record (minimum of  
 147 a year), adequate flux footprints representing typical urban neighborhoods, and the avail-  
 148 ability of observed precipitation and latent heat fluxes. All sites are located in reason-  
 149 ably flat terrain. Most sites were located in mid-latitude climates, except Mexico City  
 150 that has a subtropical climate and Singapore with a tropical climate. Helsinki, Łódź and  
 151 Seoul have a continental climate. Vegetation fractions in the associated footprints vary  
 152 in the range of 6–56%.

153 Observations were reported in averaging periods of 10–30 min depending on the  
 154 measurement protocol of each site. In this study, hourly averages were used to determine  
 155 the timing of rainfall and 24-hour averages were used for the recession analysis. For all  
 156 sites the quality control of the observed heat fluxes was performed by individual researchers  
 157 responsible for their ET flux observation site. Although the exact methodology of the  
 158 quality control differs per site, all fluxes have been properly tested in accordance with  
 159 procedures published in literature (Aubinet et al., 2012).

160 Following Teuling et al. (2006), the change in landscape dynamic storage ( $S$ ) with  
 161 time  $t$  is given by:

$$162 \quad \frac{dS(t)}{dt} = P(t) - q(t) - ET(t) \quad (1)$$

163 where  $P$  is precipitation and  $q$  is drainage/runoff, all in  $\text{mm d}^{-1}$ . During multi-day  
 164 drydowns with no rain, both  $P$  and  $q$  typically become much smaller than the other terms.  
 165 Neglecting them reduces Equation 1 to:

$$166 \quad \frac{dS(t)}{dt} = -ET(t) \quad (2)$$

167 In conditions of water-limitation, daily ET becomes a function of (soil moisture)  
 168 storage. This dependency is often assumed to be linear (Williams & Albertson, 2004;  
 169 Dardanelli et al., 2004):

$$170 \quad ET(t) = f(S(t)) = cS(t) \quad (3)$$

171 in which  $c = 1/\lambda$  is a proportionality constant. Combining Eq. 2 and Eq. 3 and  
 172 solving the differential equation leads to an exponential response of ET (Williams & Al-  
 173 bertson, 2004; Dardanelli et al., 2004):

$$174 \quad ET(t) = ET_0 \exp\left(-\frac{t - t_0}{\lambda}\right) \quad (4)$$

**Table 1.** Summary of the measurement sites and the outcomes of the regression. The climate statistics are long-term means (1999-2019). The start and end of the indicated ranges for the parameters are respectively the 5<sup>th</sup> and 95<sup>th</sup> percentile of the median distribution from the bootstrapping re-samples. The value in brackets is the median itself. (LCZ: 1 = compact high-rise, 2 = compact mid-rise, 3 = compact low-rise, 5 = open mid-rise, 6 = open low-rise,  $F_v$ : surface fraction covered by vegetation in a 500 m radius around the measurement site,  $z_s$ : height of sensors above ground level,  $z_H$ : mean building height,  $ET_0$ : initial evapotranspiration,  $\lambda$ :  $e$ -folding timescale,  $t_{\frac{1}{2}}$ : half-life,  $S_0$ : effective, dynamic water storage capacity)

City	Lat. (deg)	Lon. (deg)	Köppen-Geiger climate	Avg. temp. (deg C)	Ann. prec. (mm)	LCZ	$F_v$ (%)	$z_s$ (m)	$z_H$ (m)	Start	End	Source	Dry-down Days	$ET_0$ (mm d <sup>-1</sup> )	$\lambda$ (day)	$t_{\frac{1}{2}}$ (day)	$S_0$ (mm)
Amsterdam	52.37	4.89	Cfb	9.2	805	2	15	40	14	05/2018	10/2020	Ronda et al. (2017)	14	0.99-2 (1.5)	3.4-7.3 (3.8)	2.4-10 (2.6)	5.6-17 (6.7)
Arnhem	51.98	5.92	Cfb	9.4	778	2	12	23	11	05/2012	12/2016	Steenveeld et al. (2019)	48	0.62-0.95 (0.73)	2.6-4.6 (3.3)	1.8-3.2 (2.3)	2.4-3.9 (3.1)
Basel (AESC)	47.55	7.60	Cfb	10	778	2	27	39	17	06/2009	12/2020	Jacobs et al. (2015)	125	0.76-1 (0.83)	4.4-5.7 (5)	3.1-3.9 (3.5)	3.5-4.8 (4)
Basel (KLIN)	47.56	7.58	Cfb	10	778	2	27	41	17	05/2004	12/2020	Lietzke et al. (2015)	160	0.9-1.2 (1)	5-7 (5.7)	3.5-4.9 (3.9)	4.7-7.7 (6.1)
Berlin (ROTH)	13.32	52.46	Cfb	9.1	570	6	56	40	17	06/2018	09/2020	Schmütz et al. (2016)	8	0.46-0.95 (0.74)	4.1-12 (6.7)	2.8-8.1 (4.7)	2-9.7 (4.9)
Berlin (TUCC)	13.33	52.51	Cfb	9.1	570	5	31	56	20	07/2014	09/2020	Vulova et al. (n.d.)	38	0.31-0.78 (0.47)	3.3-5.1 (3.9)	2.3-3.5 (2.7)	1.2-3.6 (2.7)
Helsinki	60.33	24.96	Dfb	5.1	650	6	54	31	20	01/2006	12/2018	Vesala et al. (2008)	45	1.1-1.8 (1.6)	3.7-5.3 (4.3)	2.5-4 (3)	5.6-11 (7.8)
Lódz	51.76	19.45	Dfb	7.9	564	5	31	37	11	07/2006	09/2015	Karsisto et al. (2016)	59	0.74-1.4 (1)	3.6-5.3 (4.5)	2.5-3.8 (3.1)	3.4-6.7 (4.2)
Melbourne (Preston)	-37.73	145.01	Cfb	14.8	666	5	38	40	6	08/2003	11/2004	Fortuniak et al. (2013)	3	0.55-2.1 (1.5)	2.6-14 (9)	1.8-9.5 (6.2)	5-21 (5.5)
Mexico City	19.40	-99.18	Cwb	15.9	625	2	6	37	9.7	06/2011	09/2012	Coutts et al. (2007a)	8	0.69-1.5 (1.2)	5.4-17 (11)	3.8-11 (7.6)	5.8-22 (9.5)
Seoul	37.54	127.04	Dwa	11.9	1373	1	40	30	20	03/2015	02/2016	Velasco et al. (2014)	11	0.74-1.7 (1.1)	2.8-11 (6.7)	2-7.3 (4.7)	3.1-9.9 (6.7)
Singapore	1.31	103.91	Af	26.8	2378	3	15	24	10	03/2013	03/2014	Hong et al. (2019)	7	1.2-1.6 (1.3)	7-20 (10)	4.8-14 (7.2)	8.7-24 (12)
Vancouver	49.23	-123.08	Csb	9.9	1283	6	35	28	5	05/2008	07/2017	Velasco et al. (2013)	63	1-1.4 (1.2)	6.8-9.1 (7.7)	4.7-6.3 (5.4)	6.6-8.9 (7.7)

175 where  $\lambda$  is the  $e$ -folding timescale (i.e. the time over which ET is reduced by 63%),  
 176 and  $ET_0$  the initial ET. With these parameters the total dynamic storage volume  $S_0$  in  
 177 mm that would be depleted during a complete dry down ( $t \rightarrow \infty$ ) is given by:

$$178 \quad S_0 = \int_{t_0}^{\infty} ET(t)dt = \lambda ET_0. \quad (5)$$

179 so that  $S_0$  can be estimated using only ET observations. To estimate the parameters  
 180  $\lambda$  and  $ET_0$ , we identified all periods without precipitation for at least three continuous  
 181 days, since three data points are the minimum requirement for an exponential fit (Fig-  
 182 ure 1). We only consider the first ten days of the drydowns to reduce the influence of  
 183 the tail on  $ET_0$ , and to limit the contribution of garden irrigation to ET. In order to pre-  
 184 serve the information in ET during the first hours after rainfall (in case of low  $\lambda$ ), we  
 185 start the 24-hour averaging bins directly after the rainfall event, regardless of its mag-  
 186 nitude. The bin-average is assigned to the middle of the day (e.g. the first bin is assigned  
 187 to 0.5 day since rainfall). We exclude hours with an average shortwave incoming radi-  
 188 ation below  $10 \text{ W m}^{-2}$  (i.e. nighttime), since during the night ET tends to be low. Only  
 189 bins with at least 70% of data for daytime hours were analyzed, and no gap-filling was  
 190 applied. The effect of implementing the threshold instead of requiring 100% was tested  
 191 for the monitoring sites in Arnhem and Helsinki. We found that while sample size in-  
 192 creased by 53 and 27% respectively, the median of the water storage capacities only changed  
 193 by 6 and 3%. Given the minimal effect on the results and potential to increase the sam-  
 194 ple size, the threshold provides more information especially regarding cities with a shorter  
 195 measurement period without compromising the results.

196 The ET observations were transformed by taking the natural logarithm to acquire  
 197 a linear relation based on Equation 4, which is fitted through every individual drydown  
 198 with the method of least squares obtaining  $\lambda$  and  $ET_0$ . With increasing  $R^2$ , the para-  
 199 meters converge until an  $R^2$  of 0.3 (not shown), which is thus our minimum requirement.  
 200 In addition, the parameters are required to be physically plausible meaning that  $\lambda$  and  
 201  $ET_0$  have to be positive, and below 80 days respectively  $10 \text{ mm d}^{-1}$ . Also, the average  
 202 temperature during a drydown needs to exceed  $0^\circ\text{C}$  to exclude snow conditions, which  
 203 is strict enough, confirmed by a double check against snow records. To quantify the un-  
 204 certainty of the estimated parameters complying with all criteria, we applied bootstrap-  
 205 ping using 5000 re-samples containing 90% of the estimates. The confidence interval is  
 206 defined as the 5<sup>th</sup> and 95<sup>th</sup> percentile of the median distribution from the re-samples.  
 207 With  $\lambda$  and  $ET_0$  the storage capacity is calculated according to Equation 5 (shaded area  
 208 in Figure 1). The calculated storage corresponds to the total storage capacity, when the  
 209 storage capacity is assumed to be completely filled after every rainfall event. Drydowns  
 210 occurring during all seasons are included and analyzed for a seasonal effect, since the wa-  
 211 ter storage available to the atmosphere may change due to for example leaf phenology.  
 212 For both parameters and  $S_0$ , we investigate the relation to Köppen climate, LCZ and  
 213 vegetation fraction. To investigate the possible impact of day-to-day variation or change  
 214 in energy availability on the results, we repeated the recession analysis based on evap-  
 215 orative fraction (Gentine et al., 2007) multiplied by the average available energy over the  
 216 drydown, which we included in the supplementary information (Table S1 and Figure S1  
 217 and S2).

### 218 3 Results

219 In Figure 2, the individual drydowns (in grey) show a good resemblance of the char-  
 220 acteristic behaviour of the recession confirming the exponential behaviour. In general,  
 221 ET is quickly decaying after rainfall in all LCZ's represented in our sample, indicating  
 222 urban ET is generally strongly limited by water availability even on the first day after  
 223 rainfall. As all cities respond similarly, this confirms the qualitative, decaying relation

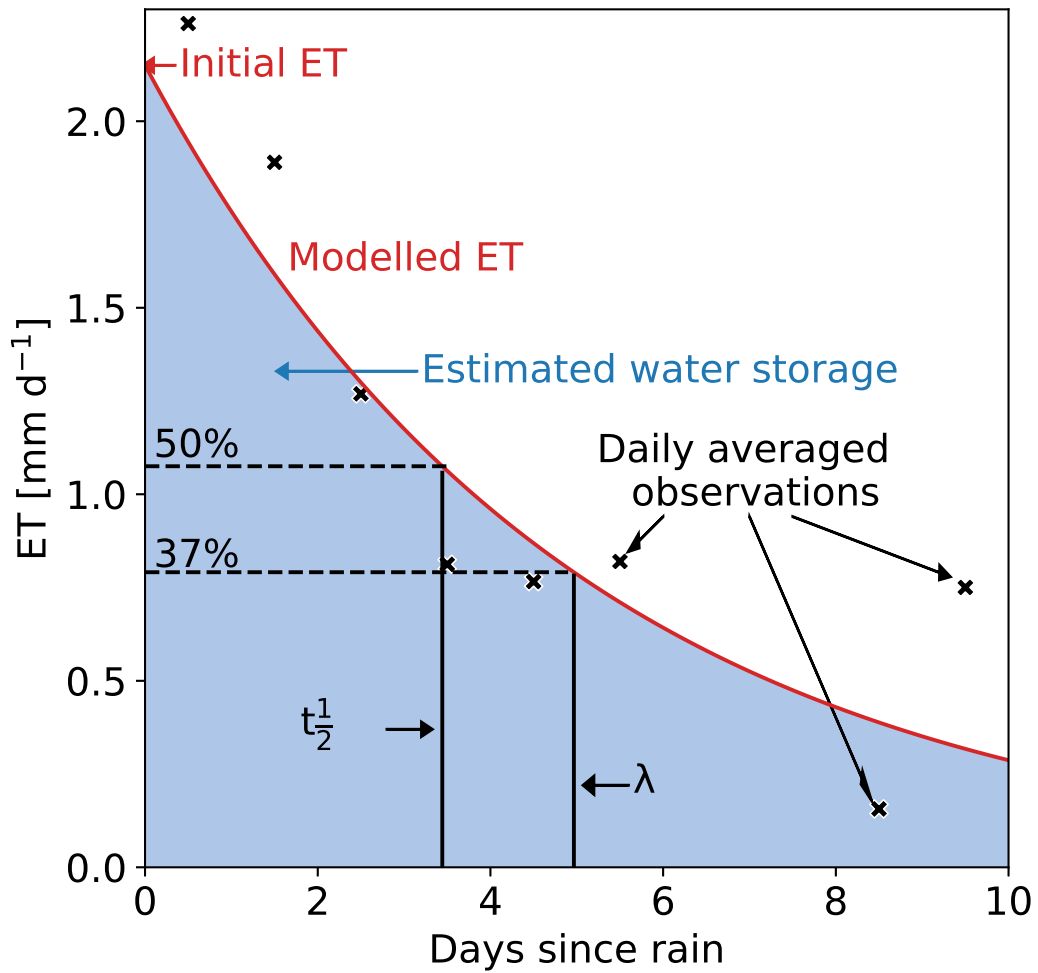


**Figure 1.** Illustration of the recession analysis. Daily averaged ET versus the number of days since the last precipitation for an example drydown from the Seoul data set with the fitted recession curve. Note that the fit was obtained by a linear fit on log-transformed data (see Data and Methods). In the figure the parameters are indicated.

224 during a drydown. The uncertainty is visibly higher in cities with shorter measurement  
 225 periods, since shorter periods inevitably mean smaller samples of drydowns. For Arn-  
 226 hem, Basel (AESC and KLIN), Berlin (Roth and TUCC), Helsinki, Łódź and Vancou-  
 227 ver, observations are available for more than two full years resulting in narrow uncer-  
 228 tainty bands. In contrast to the uncertainty bands for the sites with records of less than  
 229 two years (Amsterdam, Melbourne, Mexico City, Seoul and Singapore), which are as wide  
 230 as the range of observations. In some panels (e.g. Amsterdam and Helsinki), we observe  
 231 two groups of curves with distinct slopes, for which we found no explanation in season-  
 232 ality, temperature and pre-drydown rainfall (amount and timing). When vegetation is  
 233 irrigated in summer, irregularly high ET values can occur long after rainfall (see for ex-  
 234 amples Helsinki and Vancouver).

235 In Table 1, an overview of the parameters is given for the 589 drydowns that com-  
 236 plied with all criteria. Of the total number of 1611 drydowns, 537 are excluded because  
 237 of a negative  $\lambda$  and 74 because of a  $\lambda$  above 80 days. All drydowns had a positive  $ET_0$ ,  
 238 and only one exceeded  $10 \text{ mm d}^{-1}$ . Snow conditions influenced 133 drydowns, which are  
 239 thus excluded. Finally, 714 drydowns did not meet the minimum  $R^2$  of 0.3. The remain-  
 240 ing drydowns yielded initial evapotranspiration between  $0.3\text{--}2 \text{ mm d}^{-1}$  and  $e$ -folding timescales  
 241 between 2.5–12 days with the majority below 8 days, corresponding to half-lives of 1.7–  
 242 8.3 and 5.5 days. The related storage capacities appear to be between 1.5–20 mm with  
 243 the majority below 10 mm. As mentioned before, the length of the measurement period  
 244 determines the width of the uncertainty, which for  $S_0$  varies from 1.44 mm in Arnhem  
 245 to 16.03 mm in Mexico City (Figure 2).

246 For all sites, we find a considerable spread in the ET observations (Figure 2), which  
 247 recurs in the values found for  $S_0$ . In Figure 3,  $S_0$  is plotted against the month of the dry-  
 248 down, showing a very distinct seasonal cycle. Both  $ET_0$  and  $\lambda$ , on which  $S_0$  is based, show  
 249 similar behaviour (not shown). Melbourne is shifted to fit the seasonality, as it is situ-  
 250 ated on the southern hemisphere. Since Singapore is close to the equator, it is not ex-  
 251 pected to show seasonal effect, which is confirmed by the distribution of points in Fig-  
 252 ure 3 with no clear pattern. Any connection between  $S_0$  and site characteristics is over-  
 253 shadowed by the seasonal cycle covering the full range of  $S_0$  (Table 1), as we illustrate  
 254 in the supplementary material (Figure S3 and S4). It is unfortunately not possible to  
 255 eliminate the influence of the cycle by focusing on one season due to the steep slope, and  
 256 not by focusing on one month due to the low data density. Only after omitting half of  
 257 the cities based on the number of drydowns, a relation between  $S_0$  and site charac-  
 258 teristics is visible (Supplementary material Figure S5).

## 259 4 Discussion

260 In contrast with the results from this study found in urban areas, Teuling et al. (2006)  
 261 found timescales ranging from 15–35 days and storage varying between 30 and 150 mm  
 262 for forests and grassland with a similar methodology. When the urban parameter val-  
 263 ues found in this study are compared with these timescales and storage capacities (2.5–  
 264 12 days and 1.5–20 mm), it is clear that both the timescales and storage capacities are  
 265 higher in rural areas. McColl et al. (2017) have analyzed soil moisture drydowns in a global  
 266 study using satellite data with a resolution too coarse to explicitly resolve individual cities,  
 267 thus resembling rural values. Although their timescales with values from 2–20 days are  
 268 closer to ours, it must be noted the temporal resolution is one in every three days and  
 269 their observations only regard the first few centimeters instead of the root zone. Also,  
 270 the satellite product in their research is known to underestimate the timescales compared  
 271 to in-situ observations (Rondinelli et al., 2015; Shellito et al., 2016). Hence, the results  
 272 show that both  $\lambda$  and  $S_0$  are an order of magnitude smaller in cities indicating shorter  
 273 timescales and lower storage capacities in urban areas regardless of their climate and veg-  
 274 etation fraction.

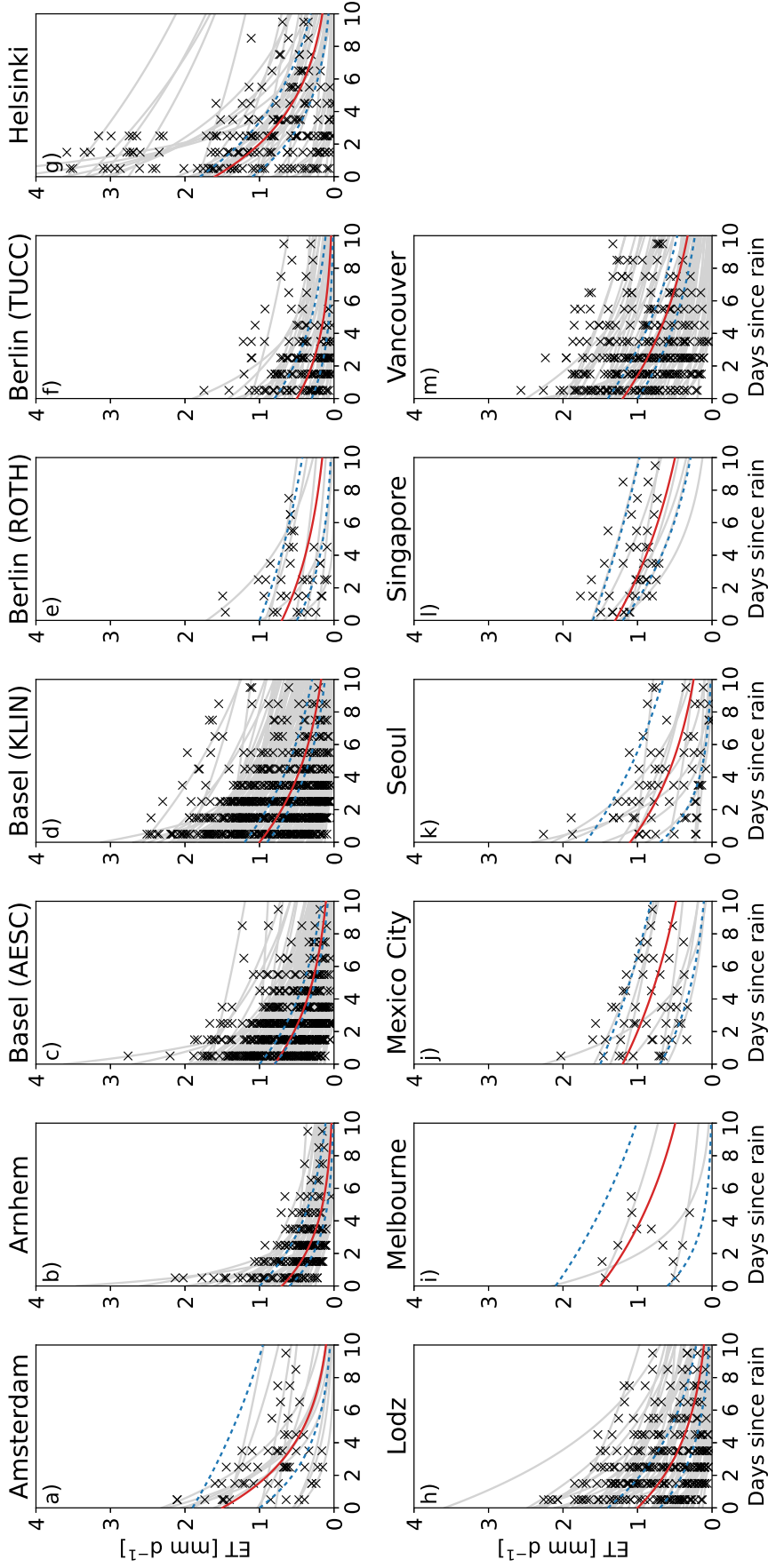


**Figure 2.** Daily average  $ET$  versus the day after the last precipitation with in red (continuous) the recession curve using the median parameter values, in blue (dotted) the 5<sup>th</sup> and 95<sup>th</sup> percentile of the median distribution from the bootstrapping re-samples, and in light grey all individual drydowns. The parameters of the fitted curves are shown in Table 1

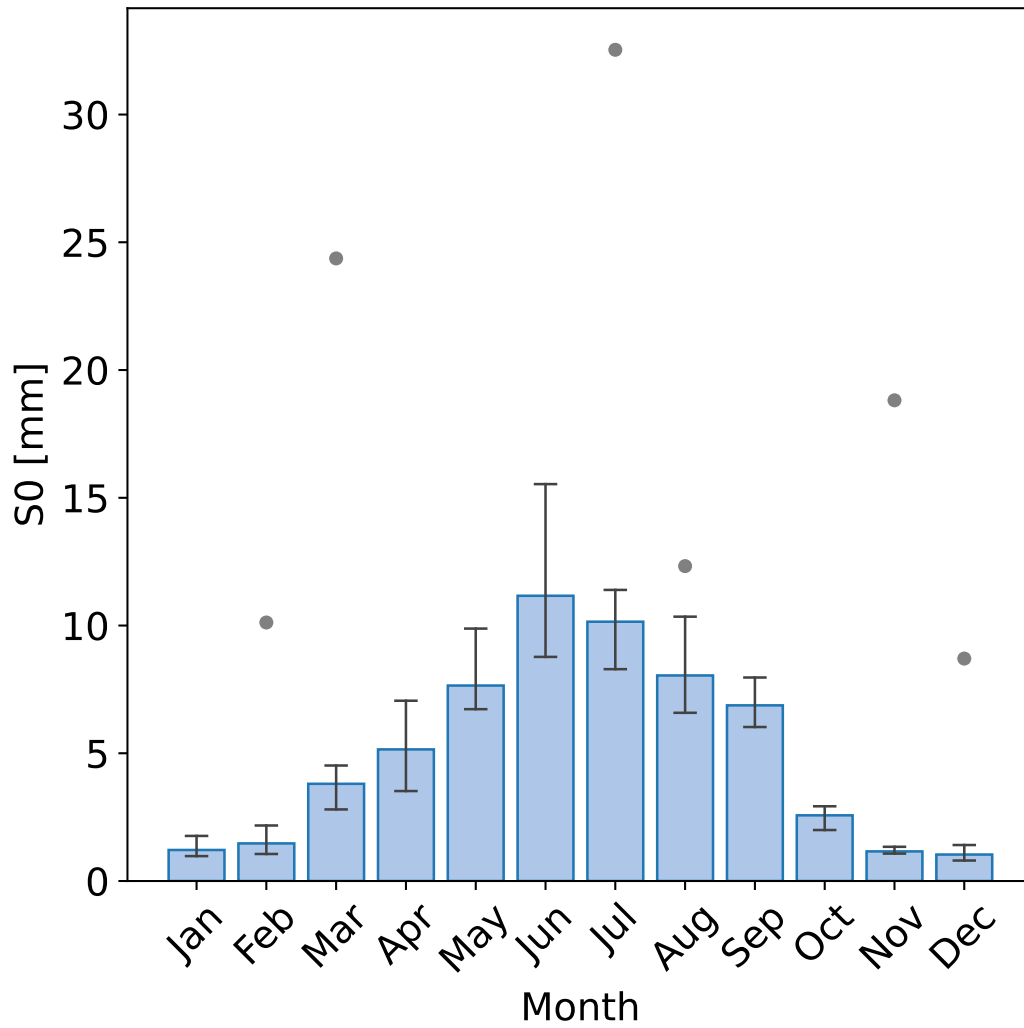


**Figure 3.** The seasonal cycle of  $S_0$  for the sites on the northern hemisphere (Melbourne is included shifted by half a year) in blue and for Singapore as grey dots. The uncertainty is determined similarly as in Figure 2.

275 The applied methodology implies a set of assumptions and limitations that con-  
276 fine its utilization. Since the method is observation-based, the reliability of the measure-  
277 ments is an important factor in this confinement. Eddy covariance is a sophisticated method  
278 for measuring fluxes, but comes with a set of potential challenges in cities (Velasco &  
279 Roth, 2010; Feigenwinter et al., 2012; Järvi et al., 2018). By carefully selecting locations  
280 and applying quality control, these problems are minimized. All sites have an observa-  
281 tion height well above the mean building height (see Table 1), and measure in the well-  
282 mixed inertial sublayer. This reduces the variability in flux measurements in response  
283 to the heterogeneity of the monitored footprint, which is induced by the many, unevenly  
284 distributed surfaces with different characteristics and water storage capacities in the ur-  
285 ban landscape. The only site in this research that includes a non-homogeneous footprint  
286 is Seoul, for which the observations are filtered by wind direction to exclude a nearby  
287 forest. Additionally, the long bins and quality control keep the influence of sudden fluctu-  
288 ations to a minimum.

289 Interception ET was an important consideration in the design of the methodology,  
290 since the high ET during the first day of a drydown can be largely attributed to this phe-  
291 nomenon (Savenije, 2004). Interception ET is a concept originally developed for forest  
292 environments, where interception is defined as water intercepted by the canopy. How-  
293 ever, the concept can also be applied in urban environments with the more general def-  
294 inition of a temporary storage space only filled directly after rainfall (e.g. Grimmond &  
295 Oke, 1991; Gerrits, 2010; Oke et al., 2017). The volume of this temporary space is af-  
296 fected by urban design choices, such as the use of flat or sloping roofs. In order to cap-  
297 ture the peak at the beginning of the recession caused by interception ET, the starting  
298 time of the 24-hour bins is not fixed but made dependent on rainfall, which can be dur-  
299 ing either day or night. Due to a lack of energy availability at night, more water may  
300 be drained and thus less interception might be evaporated. Since all parameters are in-  
301 dependent of the starting hour of the bins (not shown), a bias due to the starting hour  
302 can be ruled out.

303 Although ET is expected to behave as described in Equation 4, the anthropogenic  
304 moisture flux does not necessarily follow this equation. In urban areas, the anthropogenic  
305 moisture flux can contribute substantially to ET, in particular during long dry periods  
306 (C. Grimmond & Oke, 1986; Moriwaki et al., 2008; Miao & Chen, 2014). This moisture  
307 flux includes processes like transport, heating, cooling (indoor), human metabolism and  
308 irrigation, which do not directly depend on rainfall. We expect variations in daily av-  
309 erages of these processes, except for irrigation, to be negligible during one drydown. We  
310 have tried to capture these flux by adding a constant base term to Equation 4, but this  
311 strongly increased the number of drydowns yielding physically unfeasible parameters.  
312 Therefore, we conclude that including this part of the anthropogenic moisture flux would  
313 not improve the results. As mentioned earlier, irrigation cannot be expected to be con-  
314 stant, while in some cities (e.g. Vancouver (C. Grimmond & Oke, 1986; Järvi et al., 2011)  
315 and Melbourne (Barker et al., 2011)) its contribution to ET is considerable. Two choices  
316 in the methodology prevent irrigation from affecting the results. The first one being the  
317 maximum duration of a drydown of 10 days, and the second being the requirement that  
318 the  $R^2$  has to be above 0.3, which is not achieved if ET rises due to irrigation.

319 The methodology assumes that at the start of a drydown the storage capacity is  
320 completely full. A partly empty storage capacity would lead to an underestimation of  
321 the capacity, as less water is available for ET. We have compared the magnitude of the  
322 rain event before a drydown with the resulting parameters and found no correlation. Since  
323 the storage can be refilled by a series of events separated by dry days, we plotted the found  
324 parameters against the Antecedent Precipitation Index (API) (Fedora & Beschta, 1989).  
325 The API takes into account rainfall occurring during preceding days (here limited to 20),  
326 but also shows no correlations with the parameters. Therefore, the assumption of a com-

327 pletely filled storage is tangible and no selection has been performed based on rainfall  
328 event size.

329 The small storage capacity in cities shows their water balance is altered. Despite  
330 the limitations of the methodology discussed above, the provided first estimates show  
331 the clear contrast between water storage capacity in urban and rural areas. The presented  
332 water storage estimation method has potential to offer an intriguing comparative anal-  
333 yses between less distinctly different urban sites. The data presented here are not suf-  
334 ficient to substantiate, but do indicate their existence. In order to coin the larger poten-  
335 tial and establish empirical relations between site characteristics and storage capacity,  
336 future research will need to focus on including longer records from more cities and ap-  
337 plying soil moisture observations as a reference. The first is because urban flux records  
338 are scarce both in number and length, as was previously indicated by Grimmond and  
339 Christen (2012), but the availability is improving. Additionally, very wet climates, such  
340 as in Singapore, only sporadically satisfy the conditions of the methodology increasing  
341 the necessity of long observational records. The second, soil moisture, are available for  
342 only three sites in this study (Berlin, Singapore and Vancouver), but could provide the  
343 opportunity to estimate storage conditions. To establish robust relations, future research  
344 will need to include many more cities with records of at least two years.

## 345 5 Conclusion

346 The timescales of ET recession found in urban environments are considerably shorter  
347 than in rural environments. This is related to the storage capacity, which is also found  
348 to be lower. Timescales of cities are within 2.5–12 days with the majority below 8 days  
349 and storage capacities range between 1.5–20 mm with the majority below 10 mm. Both  
350 are an order of magnitude smaller than the values found in rural areas. We were unable  
351 to analyze differences between cities to vegetation fraction, local climate zone or climate  
352 for two reasons. Firstly, a very strong seasonal cycle in the storage capacities as strong  
353 as the total found variation. Secondly, the number of sites is limited, for which no more  
354 than one year of data is available for about half of them. When provided with more data,  
355 the presented water storage capacity method does have the potential to establish robust  
356 empirical relations explaining the differences between cities.

## 357 Acknowledgments

358 Harro Jongen acknowledges this research was supported by the WIMEK PhD grant 2020.  
359 The observations in the Amsterdam Atmospheric Monitoring Supersite have been finan-  
360 cially supported by the Amsterdam Institute for Advanced Metropolitan Solutions (AMS  
361 Institute, project VIR16002). Gert-Jan Steeneveld acknowledges funding from the Nether-  
362 lands Organisation for Scientific Research (NWO) Project 864.14.007. The observations  
363 in Arnhem are part of “Climate Proof Cities”, carried out in the second phase of the  
364 Knowledge for Climate Program, co-financed by the Dutch Ministry of Infrastructure  
365 and the Environment. It is also part of the strategic research program KBIV ‘Sustain-  
366 able spatial development of ecosystems, landscapes, seas and regions’, funded by the Dutch  
367 Ministry of Economic Affairs, Agriculture and Innovation, and carried out by Wagenin-  
368 gen University and Research Centre (Project KB-14-002-005). Fred Meier acknowledges  
369 funding for instrumentation of the Urban Climate Observatory (UCO) Berlin from Deutsche  
370 Forschungsgemeinschaft (DFG) grant SCHE 750/8 and SCHE 750/9 within Research  
371 Unit 1736 “Urban Climate and Heat Stress in Mid Latitude Cities in View of Climate  
372 Change (UCaHS)” and the research programme “Urban Climate Under Change ([UC]<sup>2</sup>)”,  
373 funded by the German Ministry of Research and Education (FKZ 01LP1602A). For Helsinki  
374 we thank the Academy of Finland funded ICOS-Finland and CarboCity (grant no. 321527).  
375 The flux tower in Mexico City was supported by the National Institute of Ecology and  
376 Climate Change (INECC) and Mexico City’s Secretariat for the Environment through  
377 the Molina Center for Energy and the Environment (MCE2). The site in Seoul was sup-

378 ported by a National Research Foundation of Korea Grant from the Korean Government  
 379 (MSIT) ( NRF-2018R1A5A1024958 ). The operation of Singapore’s flux tower was sup-  
 380 ported by the National Research Foundation and the National University of Singapore  
 381 (research grant R-109-000-091-112). Andreas Christen acknowledges support for the Van-  
 382 couver observations through two Discovery Grants of the Natural Science and Engineer-  
 383 ing Research Council of Canada (NSERC), the Canada Foundation for Innovation (CFI)  
 384 and the Canadian Foundation for Climate and Atmospheric Sciences (CFCAS). The data  
 385 that support the findings of this study are openly available in data.4tu at <http://doi.org/10.4121/13686973>.  
 386 (will be available upon acceptance)

## 387 References

- 388 Arnold Jr, C. L., & Gibbons, C. J. (1996). Impervious surface coverage: the emer-  
 389 gence of a key environmental indicator. *Journal of the American planning As-*  
 390 *sociation*, *62*(2), 243–258.
- 391 Aubinet, M., Vesala, T., & Papale, D. (2012). *Eddy covariance: a practical guide to*  
 392 *measurement and data analysis*. Springer Science & Business Media.
- 393 Avissar, R. (1992). Conceptual aspects of a statistical-dynamical approach to repre-  
 394 sent landscape subgrid-scale heterogeneities in atmospheric models. *Journal of*  
 395 *Geophysical Research: Atmospheres*, *97*(D3), 2729–2742.
- 396 Barker, F., Faggian, R., & Hamilton, A. J. (2011). A history of wastewater irrigation  
 397 in Melbourne, Australia. *Journal of Water Sustainability*, *1*(2), 31–50.
- 398 Boese, S., Jung, M., Carvalhais, N., Teuling, A. J., & Reichstein, M. (2019).  
 399 Carbon–water flux coupling under progressive drought. *Biogeosciences*, *16*(13),  
 400 2557–2572.
- 401 Brutsaert, W., & Nieber, J. L. (1977). Regionalized drought flow hydrographs from  
 402 a mature glaciated plateau. *Water Resources Research*, *13*(3), 637–643.
- 403 Christen, A., Coops, N., Crawford, B., Kellett, R., Liss, K., Olchovski, I., ... Voogt,  
 404 J. (2011). Validation of modeled carbon-dioxide emissions from an urban  
 405 neighborhood with direct eddy-covariance measurements. *Atmospheric Envi-*  
 406 *ronment*, *45*(33), 6057–6069.
- 407 Christen, A., & Vogt, R. (2004). Energy and radiation balance of a central European  
 408 city. *International Journal of Climatology: A Journal of the Royal Meteorologi-*  
 409 *cal Society*, *24*(11), 1395–1421.
- 410 Coutts, A. M., Beringer, J., & Tapper, N. J. (2007a). Characteristics influencing the  
 411 variability of urban co2 fluxes in Melbourne, Australia. *Atmospheric Environ-*  
 412 *ment*, *41*(1), 51–62.
- 413 Coutts, A. M., Beringer, J., & Tapper, N. J. (2007b). Impact of increasing urban  
 414 density on local climate: Spatial and temporal variations in the surface en-  
 415 ergy balance in Melbourne, Australia. *Journal of Applied Meteorology and*  
 416 *Climatology*, *46*(4), 477–493.
- 417 Dardanelli, J. L., Ritchie, J., Calmon, M., Andriani, J. M., & Collino, D. J. (2004).  
 418 An empirical model for root water uptake. *Field Crops Research*, *87*(1), 59–  
 419 71.
- 420 Ennos, R. (2010). Urban cool. *Physics World*, *23*(08), 22.
- 421 Fedora, M., & Beschta, R. (1989). Storm runoff simulation using an antecedent pre-  
 422 cipitation index (API) model. *Journal of hydrology*, *112*(1-2), 121–133.
- 423 Feigenwinter, C., Vogt, R., & Christen, A. (2012). Eddy covariance measurements  
 424 over urban areas. In M. Aubinet, T. Vesala, & D. Papale (Eds.), *Eddy co-*  
 425 *variance a practical guide to measurement and data analysis* (p. 377-397).  
 426 Dordrecht: Springer Netherlands.
- 427 Fletcher, T. D., Andrieu, H., & Hamel, P. (2013). Understanding, management  
 428 and modelling of urban hydrology and its consequences for receiving waters: A  
 429 state of the art. *Advances in water resources*, *51*, 261–279.
- 430 Fortuniak, K., Pawlak, W., & Siedlecki, M. (2013). Integral turbulence statistics

- 431 over a central European city centre. *Boundary-layer meteorology*, 146(2), 257–  
432 276.
- 433 Gabriel, K. M., & Endlicher, W. R. (2011). Urban and rural mortality rates dur-  
434 ing heat waves in Berlin and Brandenburg, Germany. *Environmental pollution*,  
435 159(8-9), 2044–2050.
- 436 Gaines, J. M. (2016). Water potential. *Nature*, 531(7594 S1), S54–S54.
- 437 Gallo, K., McNab, A., Karl, T. R., Brown, J. F., Hood, J., & Tarpley, J. (1993).  
438 The use of a vegetation index for assessment of the urban heat island effect.  
439 *Remote Sensing*, 14(11), 2223–2230.
- 440 Gash, J., Rosier, P., & Ragab, R. (2008). A note on estimating urban roof runoff  
441 with a forest evaporation model. *Hydrological Processes: An International*  
442 *Journal*, 22(8), 1230–1233.
- 443 Gasparri, A., Guo, Y., Sera, F., Vicedo-Cabrera, A. M., Huber, V., Tong, S., ...  
444 others (2017). Projections of temperature-related excess mortality under  
445 climate change scenarios. *The Lancet Planetary Health*, 1(9), e360–e367.
- 446 Gentine, P., Entekhabi, D., Chehbouni, A., Boulet, G., & Duchemin, B. (2007).  
447 Analysis of evaporative fraction diurnal behaviour. *Agricultural and forest*  
448 *meteorology*, 143(1-2), 13–29.
- 449 Gerrits, A. M. J. (2010). *The role of interception in the hydrological cycle* (Unpub-  
450 lished doctoral dissertation). TU Delft.
- 451 Graham, P., Maclean, L., Medina, D., Patwardhan, A., & Vasarhelyi, G. (2004). The  
452 role of water balance modelling in the transition to low impact development.  
453 *Water Quality Research Journal*, 39(4), 331–342.
- 454 Grimmond, & Christen, A. (2012). Flux measurements in urban ecosystems.  
455 *FluxLetter*.
- 456 Grimmond, & Oke, T. R. (1991). An evapotranspiration-interception model for ur-  
457 ban areas. *Water Resources Research*, 27(7), 1739–1755.
- 458 Grimmond, C., & Oke, T. R. (1986). Urban water balance: 2. results from a sub-  
459 urb of Vancouver, British Columbia. *Water Resources Research*, 22(10), 1404–  
460 1412.
- 461 Hamdi, R., Termonia, P., & Baguis, P. (2011). Effects of urbanization and climate  
462 change on surface runoff of the Brussels Capital Region: a case study using an  
463 urban soil–vegetation–atmosphere-transfer model. *International Journal of*  
464 *Climatology*, 31(13), 1959–1974.
- 465 Harshan, S., Roth, M., Velasco, E., & Demuzere, M. (2017). Evaluation of an urban  
466 land surface scheme over a tropical suburban neighborhood. *Theoretical and*  
467 *applied climatology*, 133(3-4), 867–886.
- 468 Hong, J.-W., Hong, J., Chun, J., Lee, Y. H., Chang, L.-S., Lee, J.-B., ... Joo, S.  
469 (2019). Comparative assessment of net CO<sub>2</sub> exchange across an urbanization  
470 gradient in Korea based on eddy covariance measurements. *Carbon balance and*  
471 *management*, 14(1), 13.
- 472 Hong, J.-W., Lee, S.-D., Lee, K., & Hong, J. (2020). Seasonal variations in the  
473 surface energy and CO<sub>2</sub> flux over a high-rise, high-population, residential urban  
474 area in the East Asian monsoon region. *International Journal of Climatology*.
- 475 Huntington, T. G. (2006). Evidence for intensification of the global water cycle: re-  
476 view and synthesis. *Journal of Hydrology*, 319(1-4), 83–95.
- 477 Jacobs, C., Elbers, J., Broelsma, R., Hartogensis, O., Moors, E., Márquez, M. T. R.-  
478 C., & van Hove, B. (2015). Assessment of evaporative water loss from Dutch  
479 cities. *Building and environment*, 83, 27–38.
- 480 Järvi, L., Grimmond, C., & Christen, A. (2011). The surface urban energy and wa-  
481 ter balance scheme (suews): Evaluation in Los Angeles and Vancouver. *Journal*  
482 *of Hydrology*, 411(3-4), 219–237.
- 483 Järvi, L., Rannik, U., Kokkonen, T. V., Kurppa, M., Karppinen, A., Kouznetsov,  
484 R. D., ... Wood, C. R. (2018). Uncertainty of eddy covariance flux measure-  
485 ments over an urban area based on two towers. *Atmospheric Measurement*

- 486 *Techniques*, 11(10), 5421–5438. Retrieved from [https://amt.copernicus](https://amt.copernicus.org/articles/11/5421/2018/)  
 487 [.org/articles/11/5421/2018/](https://amt.copernicus.org/articles/11/5421/2018/) doi: 10.5194/amt-11-5421-2018
- 488 Jin, L., Schubert, S., Fenner, D., Meier, F., & Schneider, C. (2020). Integration  
 489 of a building energy model in an urban climate model and its application.  
 490 *Boundary-Layer Meteorology*, 1–33.
- 491 Karsisto, P., Fortelius, C., Demuzere, M., Grimmond, C. S. B., Oleson, K.,  
 492 Kouznetsov, R., . . . Järvi, L. (2016). Seasonal surface urban energy bal-  
 493 ance and wintertime stability simulated using three land-surface models in  
 494 the high-latitude city Helsinki. *Quarterly Journal of the Royal Meteorological*  
 495 *Society*, 142(694), 401–417.
- 496 Kirchner, J. W. (2009). Catchments as simple dynamical systems: Catchment char-  
 497 acterization, rainfall-runoff modeling, and doing hydrology backward. *Water*  
 498 *Resources Research*, 45(2).
- 499 Laaidi, K., Zeghnoun, A., Dousset, B., Bretin, P., Vandentorren, S., Giraudet, E.,  
 500 & Beaudeau, P. (2011). The impact of heat islands on mortality in Paris  
 501 during the August 2003 heat wave. *Environmental health perspectives*, 120(2),  
 502 254–259.
- 503 Lietzke, B., Vogt, R., Feigenwinter, C., & Parlow, E. (2015). On the controlling  
 504 factors for the variability of carbon dioxide flux in a heterogeneous urban  
 505 environment. *International journal of climatology*, 35(13), 3921–3941.
- 506 McColl, K. A., Wang, W., Peng, B., Akbar, R., Short Gianotti, D. J., Lu, H., . . .  
 507 Entekhabi, D. (2017). Global characterization of surface soil moisture dry-  
 508 downs. *Geophysical Research Letters*, 44(8), 3682–3690.
- 509 Meili, N., Manoli, G., Burlando, P., Bou-Zeid, E., Chow, W. T., Coutts, A. M., . . .  
 510 others (2020). An urban ecohydrological model to quantify the effect of veg-  
 511 etation on urban climate and hydrology (UT&C v1. 0). *Geoscientific Model*  
 512 *Development*, 13(1), 335–362.
- 513 Meili, N., Manoli, G., Burlando, P., Carmeliet, J., Chow, W. T., Coutts, A. M., . . .  
 514 Faticchi, S. (2021a). Tree effects on urban microclimate: Diurnal, seasonal,  
 515 and climatic temperature differences explained by separating radiation, evap-  
 516 otranspiration, and roughness effects. *Urban Forestry & Urban Greening*, 58,  
 517 126970.
- 518 Meili, N., Manoli, G., Burlando, P., Carmeliet, J., Chow, W. T., Coutts, A. M., . . .  
 519 Faticchi, S. (2021b). Tree effects on urban microclimate: Diurnal, seasonal,  
 520 and climatic temperature differences explained by separating radiation, evap-  
 521 otranspiration, and roughness effects. *Urban Forestry & Urban Greening*, 58,  
 522 126970. Retrieved from [https://www.sciencedirect.com/science/article/](https://www.sciencedirect.com/science/article/pii/S1618866720307871)  
 523 [pii/S1618866720307871](https://www.sciencedirect.com/science/article/pii/S1618866720307871) doi: <https://doi.org/10.1016/j.ufug.2020.126970>
- 524 Miao, S., & Chen, F. (2014). Enhanced modeling of latent heat flux from urban  
 525 surfaces in the noah/single-layer urban canopy coupled model. *Science China*  
 526 *Earth Sciences*, 57(10), 2408–2416.
- 527 Moriwaki, R., Kanda, M., Senoo, H., Hagishima, A., & Kinouchi, T. (2008). Anthro-  
 528 pogenic water vapor emissions in Tokyo. *Water Resources Research*, 44(11).
- 529 Oke, T. R. (1982). The energetic basis of the urban heat island. *Quarterly Journal*  
 530 *of the Royal Meteorological Society*, 108(455), 1–24.
- 531 Oke, T. R., Mills, G., Christen, A., & Voogt, J. A. (2017). *Urban climates*. Cam-  
 532 bridge University Press.
- 533 Pataki, D. E., McCarthy, H. R., Litvak, E., & Pincetl, S. (2011). Transpiration  
 534 of urban forests in the Los Angeles metropolitan area. *Ecological Applications*,  
 535 21(3), 661–677.
- 536 Paul, M. J., & Meyer, J. L. (2001). Streams in the urban landscape. *Annual review*  
 537 *of Ecology and Systematics*, 32(1), 333–365.
- 538 Qin, H.-p., Li, Z.-x., & Fu, G. (2013). The effects of low impact development on ur-  
 539 ban flooding under different rainfall characteristics. *Journal of environmental*  
 540 *management*, 129, 577–585.

- 541 Ramamurthy, P., & Bou-Zeid, E. (2014). Contribution of impervious surfaces to ur-  
542 ban evaporation. *Water Resources Research*, *50*(4), 2889–2902.
- 543 Ronda, R., Steeneveld, G., Heusinkveld, B., Attema, J., & Holtslag, A. (2017). Ur-  
544 ban finescale forecasting reveals weather conditions with unprecedented detail.  
545 *Bulletin of the American Meteorological Society*, *98*(12), 2675–2688.
- 546 Rondinelli, W. J., Hornbuckle, B. K., Patton, J. C., Cosh, M. H., Walker, V. A.,  
547 Carr, B. D., & Logsdon, S. D. (2015). Different rates of soil drying after rain-  
548 fall are observed by the SMOS satellite and the south fork in situ soil moisture  
549 network. *Journal of Hydrometeorology*, *16*(2), 889–903.
- 550 Roth, M., Jansson, C., & Velasco, E. (2017). Multi-year energy balance and carbon  
551 dioxide fluxes over a residential neighbourhood in a tropical city. *International*  
552 *Journal of Climatology*, *37*(5), 2679–2698.
- 553 Sailor, D. J. (2011). A review of methods for estimating anthropogenic heat and  
554 moisture emissions in the urban environment. *International journal of clima-*  
555 *tology*, *31*(2), 189–199.
- 556 Saleem, J. A., & Salvucci, G. D. (2002). Comparison of soil wetness indices for in-  
557 ducing functional similarity of hydrologic response across sites in Illinois. *Jour-*  
558 *nal of Hydrometeorology*, *3*(1), 80–91.
- 559 Salvucci, G. D. (2001). Estimating the moisture dependence of root zone water loss  
560 using conditionally averaged precipitation. *Water Resources Research*, *37*(5),  
561 1357–1365.
- 562 Santamouris, M. (2014). Cooling the cities—a review of reflective and green roof  
563 mitigation technologies to fight heat island and improve comfort in urban  
564 environments. *Solar energy*, *103*, 682–703.
- 565 Santamouris, M. (2015). Analyzing the heat island magnitude and characteristics in  
566 one hundred Asian and Australian cities and regions. *Science of the Total En-*  
567 *vironment*, *512*, 582–598.
- 568 Savenije, H. H. (2004). The importance of interception and why we should delete the  
569 term evapotranspiration from our vocabulary. *Hydrological Processes*, *18*(8),  
570 1507–1511.
- 571 Schmutz, M., Vogt, R., Feigenwinter, C., & Parlow, E. (2016). Ten years of eddy  
572 covariance measurements in Basel, Switzerland: Seasonal and interannual vari-  
573 abilities of urban co2 mole fraction and flux. *Journal of Geophysical Research:*  
574 *Atmospheres*, *121*(14), 8649–8667.
- 575 Shellito, P. J., Small, E. E., Colliander, A., Bindlish, R., Cosh, M. H., Berg, A. A.,  
576 ... others (2016). SMAP soil moisture drying more rapid than observed in situ  
577 following rainfall events. *Geophysical research letters*, *43*(15), 8068–8075.
- 578 Starke, P., Göbel, P., & Coldewey, W. (2010). Urban evaporation rates for water-  
579 permeable pavements. *Water Science and Technology*, *62*(5), 1161–1169.
- 580 Steeneveld, G.-J., van der Horst, S., & Heusinkveld, B. (2019). *Observing the sur-*  
581 *face radiation and energy balance, carbon dioxide and methane fluxes over the*  
582 *city centre of Amsterdam*. Presented at the EGU General Assembly 2020,  
583 Online, 4–8 May 2020. doi: [https://doi-org.ezproxy.library.wur.nl/10.5194/](https://doi-org.ezproxy.library.wur.nl/10.5194/egusphere-egu2020-1547)  
584 [egusphere-egu2020-1547](https://doi-org.ezproxy.library.wur.nl/10.5194/egusphere-egu2020-1547)
- 585 Stewart, I. D., & Oke, T. R. (2012). Local climate zones for urban temperature  
586 studies. *Bulletin of the American Meteorological Society*, *93*(12), 1879–1900.
- 587 Stone Jr, B., & Rodgers, M. O. (2001). Urban form and thermal efficiency: how the  
588 design of cities influences the urban heat island effect. *American Planning As-*  
589 *sociation. Journal of the American Planning Association*, *67*(2), 186.
- 590 Taha, H. (1997). Urban climates and heat islands: albedo, evapotranspiration, and  
591 anthropogenic heat. *Energy and buildings*, *25*(2), 99–103.
- 592 Teuling, A. J., Seneviratne, S., Williams, C., & Troch, P. (2006). Observed  
593 timescales of evapotranspiration response to soil moisture. *Geophysical Re-*  
594 *search Letters*, *33*(23).
- 595 Theeuwes, N. E., Steeneveld, G.-J., Ronda, R. J., & Holtslag, A. A. (2017). A di-

- agnostic equation for the daily maximum urban heat island effect for cities in northwestern Europe. *International Journal of Climatology*, 37(1), 443–454.
- Tingsanchali, T. (2012). Urban flood disaster management. *Procedia engineering*, 32, 25–37.
- Troch, P. A., Berne, A., Bogaart, P., Harman, C., Hilberts, A. G., Lyon, S. W., . . . others (2013). The importance of hydraulic groundwater theory in catchment hydrology: The legacy of Wilfried Brutsaert and Jean-Yves Parlange. *Water Resources Research*, 49(9), 5099–5116.
- United Nations. (2018). *World urbanization prospects, the 2018 revision*. UN Department of Economic and Social Affairs.
- Velasco, E., Perrusquia, R., Jiménez, E., Hernández, F., Camacho, P., Rodríguez, S., . . . Molina, L. (2014). Sources and sinks of carbon dioxide in a neighborhood of Mexico City. *Atmospheric Environment*, 97, 226–238.
- Velasco, E., Pressley, S., Grivicke, R., Allwine, E., Molina, L. T., & Lamb, B. (2011). Energy balance in urban Mexico City: observation and parameterization during the MILAGRO/MCMA-2006 field campaign. *Theoretical and applied climatology*, 103(3-4), 501–517.
- Velasco, E., & Roth, M. (2010). Cities as net sources of co<sub>2</sub>: Review of atmospheric co<sub>2</sub> exchange in urban environments measured by eddy covariance technique. *Geography Compass*, 4(9), 1238–1259.
- Velasco, E., Roth, M., Tan, S., Quak, M., Nabarro, S., & Norford, L. (2013). The role of vegetation in the co<sub>2</sub> flux from a tropical urban neighbourhood. *Atmospheric Chemistry and Physics*.
- Vesala, T., Järvi, L., Launiainen, S., Sogachev, A., Rannik, Ü., Mammarella, I., . . . others (2008). Surface–atmosphere interactions over complex urban terrain in Helsinki, Finland. *Tellus B: Chemical and Physical Meteorology*, 60(2), 188–199.
- Vulova, S., Meier, F., Rocha, A., Quanz, J., Nouri, H., & Kleinschmit, B. (n.d.). Modeling urban evapotranspiration using remote sensing, flux footprints, and artificial intelligence.
- Wei, W., & Shu, J. (2020). Urban renewal can mitigate urban heat islands. *Geophysical Research Letters*.
- Weng, Q., Lu, D., & Schubring, J. (2004). Estimation of land surface temperature–vegetation abundance relationship for urban heat island studies. *Remote sensing of Environment*, 89(4), 467–483.
- Wetzel, P. J., & Chang, J.-T. (1987). Concerning the relationship between evapotranspiration and soil moisture. *Journal of climate and applied meteorology*, 26(1), 18–27.
- Wilby, R. L. (2007). A review of climate change impacts on the built environment. *Built environment*, 33(1), 31–45.
- Williams, C. A., & Albertson, J. D. (2004). Soil moisture controls on canopy-scale water and carbon fluxes in an African savanna. *Water Resources Research*, 40(9).
- Wong, T. H. (2006). Water sensitive urban design—the journey thus far. *Australasian Journal of Water Resources*, 10(3), 213–222.
- Zhao, L., Lee, X., Smith, R. B., & Oleson, K. (2014). Strong contributions of local background climate to urban heat islands. *Nature*, 511(7508), 216.
- Zhou, Q. (2014). A review of sustainable urban drainage systems considering the climate change and urbanization impacts. *Water*, 6(4), 976–992.
- Zhou, Q., Leng, G., Su, J., & Ren, Y. (2019). Comparison of urbanization and climate change impacts on urban flood volumes: Importance of urban planning and drainage adaptation. *Science of the Total Environment*, 658, 24–33.